

X-Ray Diffraction by Randomly Oriented Line Gratings

By R. CLARK JONES

Research Laboratory, Polaroid Corporation, Cambridge, Massachusetts, U.S.A.

(Received 9 December 1947 and in revised form 22 February 1949)

This paper contains a calculation of the X-ray diffraction pattern to be expected from a randomly oriented assemblage of line gratings. A line grating is defined as a periodic linear structure, most generally represented by a chain of similarly oriented and uniformly separated unit cells arranged along a straight line. The calculations assume that the line gratings are also randomly positioned in space, and that the number N of unit cells in each of the line gratings is the same. The corresponding result for a distribution of lengths among the line gratings, however, may be obtained by suitably averaging the result given.

The calculated pattern is compared with the corresponding patterns for ordinary three-dimensional crystals and for two-dimensional arrays, and it is shown that the pattern for the two-dimensional arrays represents a combination of the properties of the patterns for line gratings and three-dimensional crystals. A typical intensity distribution is shown, and it is found that, even for large values of N , the pattern shows a smooth distribution of diffracted intensity, except for sudden changes in the intensity at the angles which would correspond to the position of the $h00$ lines in a simple cubic lattice with the same separation between adjacent unit cells.

Introduction

The X-ray diffraction patterns obtained in as yet unpublished work by Dr Cutler D. West on certain organic polymers containing iodine and other halogens have led him to suspect that the halogen may be contained in these compounds in the form of straight chains of halogen atoms, that the directions of these chains are random, and that the separation of adjacent chains is random. Accordingly, it seemed desirable to study in detail the theoretical diffraction patterns to be expected from a random assemblage of line gratings. The present paper is devoted to this theoretical study.

A line grating is defined here as a periodic linear structure, most simply exemplified by a straight chain of uniformly spaced atoms, and most generally represented by a chain of similarly oriented unit cells arranged along a line with a constant translation vector \mathbf{a} representing the separation of adjacent unit cells. The line grating is termed a one-dimensional point grating by Compton & Allison (1935, p. 332).

Consider a line grating defined by the translation vector \mathbf{a} , whose axis makes the angle χ with the direction of propagation \mathbf{s}_0 of the original X-ray beam, as shown in Fig. 1. It has been shown by Compton & Allison that the diffracted intensity will have pronounced maxima in the directions of the generators of a certain set of cones, all of which have the direction \mathbf{a} as a symmetry axis. From the figure it is evident that the half-angles of the cones are those angles which satisfy the condition that the difference of the distances AB and CD should be a whole number, h , of wave-lengths.

Thus, the various cones may be indexed by the order h , where the integer h assumes both positive and

negative values as well as zero. Each of the cones gives rise to a ring-shaped pattern on the surface of a sphere with the line grating at the center.

The problem treated in this paper is the determination of how the ring-shaped patterns are spread out when they are produced by an assemblage of line gratings with random orientations. The results of the study are given immediately below in Part I and the derivation of the results is given in Part II.

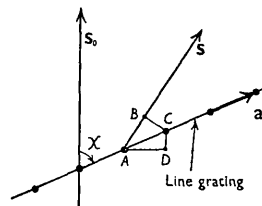


Fig. 1. Some of the vectors and co-ordinates used in the treatment. The direction indicated by the unit vector \mathbf{s}_0 is that of the undeviated X-ray beam. The line marked 'line grating' is the line along which the unit cells are located. The heavy dots along the line represent the positions of the unit cells, or, in the simple case in which the unit cell contains only one atom, the positions of the atoms.

Part I. Statement of results

The intensity of the diffracted radiation at the Bragg angle θ for a random assemblage of line gratings may be written

$$I(\theta) = \frac{I_0 e^4 N M}{m^2 c^4 R^2} \frac{1 + \cos^2 2\theta}{2} \langle F^2 \rangle_{\text{Av.}} J(\theta). \quad (1.1)$$

In this expression N is the number of unit cells in a single line grating and M is the total number of line gratings in the sample; thus NM is the total number of

unit cells in the sample. The quantity $\langle F^2 \rangle_{\Delta v}$ is the square of the structure factor of the unit cell with respect to orientation on the basis that all orientations are equally probable; this average is a function only of θ . In the important special case in which the unit cell contains only one atom, the function $\langle F^2 \rangle_{\Delta v}$ is equal to the square of the atomic scattering function $f_0(\theta)$.

It is shown in Part II that the exact expression for the function $J(\theta)$ is

$$J(\theta) = \frac{1}{N\pi z} \int_0^{\pi z} \frac{\sin^2 Nx}{\sin^2 x} dx, \quad (1.2)$$

where z is the abbreviation

$$z \equiv \frac{2a \sin \theta}{\lambda}. \quad (1.3)$$

The length a is the separation between adjacent unit cells and λ is the wave-length of the X-rays.

The expression (1.2) for $J(\theta)$ may be written in closed form in terms of trigonometric functions

$$J(\theta) = 1 + \sum_{j=1}^{N-1} \frac{2(N-j) \sin 2\pi j z}{N \cdot 2\pi j z}. \quad (1.4)$$

The expression $J(\theta)$ in this form involves a sum of N terms. The expression is thus suitable when N is small but becomes awkward to use when N becomes larger than say 4 or 5.

An approximate expression for $J(\theta)$ whose accuracy increases as N becomes larger is given by

$$J(\theta) = \frac{1}{z} \left(-\frac{1}{2} + \sum_{h=0}^{\infty} P[\pi^{\frac{1}{2}} N(z-h)] \right), \quad (1.5)$$

where the function $P[x]$ is the probability integral defined by

$$P[x] = \frac{1}{\pi^{\frac{1}{2}}} \int_{-\infty}^x e^{-z^2} dz. \quad (1.6)$$

A brief table of this function is given in Table 1.

Table 1. *Tabulation of the function $P[x]$*

x	$P[x]$	x	$P[x]$
-2.0	0.002	0.0	0.500
-1.9	0.004	0.1	0.556
-1.8	0.005	0.2	0.611
-1.7	0.008	0.3	0.664
-1.6	0.012	0.4	0.714
-1.5	0.017	0.5	0.760
-1.4	0.024	0.6	0.802
-1.3	0.033	0.7	0.839
-1.2	0.045	0.8	0.871
-1.1	0.060	0.9	0.898
-1.0	0.079	1.0	0.921
-0.9	0.102	1.1	0.940
-0.8	0.129	1.2	0.955
-0.7	0.161	1.3	0.967
-0.6	0.198	1.4	0.976
-0.5	0.240	1.5	0.983
-0.4	0.286	1.6	0.988
-0.3	0.336	1.7	0.992
-0.2	0.389	1.8	0.995
-0.1	0.444	1.9	0.996
0.0	0.500	2.0	0.998

The expression for $J(\theta)$ in (1.5) involves a sum over the various orders of the diffraction pattern rather than

the sum involved in (1.4). Accordingly, the labor of evaluating $J(\theta)$ from (1.5) is independent of the number N .

The approximate expression (1.5) may be written in the form

$$J(\theta) = \sum_{h=-\infty}^{+\infty} J_h(\theta), \quad (1.7)$$

where $J_h(\theta) = \frac{1}{2} P[\pi^{\frac{1}{2}} N(z - |h|)]/z$ ($h \neq 0$), (1.8)

and $J_0(\theta) = \{P[\pi^{\frac{1}{2}} N z] - \frac{1}{2}\}/z$. (1.9)

In this form each of the $J_h(\theta)$'s represents the contribution to the total intensity of the ring-shaped pattern of order h which was described in the Introduction. Because J_{-h} is equal to J_h , (1.7) may also be written in the form

$$J(\theta) = J_0(\theta) + 2 \sum_{h=1}^{\infty} J_h(\theta). \quad (1.10)$$

This form indicates clearly the fact that the non-zero orders have a weight of two relative to a weight of unity for the zero order.

In order to compare the pattern of randomly oriented line gratings with the corresponding patterns of randomly oriented three-dimensional crystals and of randomly oriented two-dimensional arrays, the intensity distributions corresponding to a single order for each of these three cases, three-dimensional crystal, two-dimensional array and line grating, are shown in Figs. 2(a-c). (The distribution for the random assemblage of two-dimensional arrays has been plotted from the theory developed by Warren (1941).)

In these figures the intensity distributions are those due only to the factor $J(\theta)$ and do not include the effect on the intensity distribution of the polarization factor, $\frac{1}{2}(1 + \cos^2 2\theta)$, or the structure factor, $\langle F^2 \rangle_{\Delta v}$. In each case the patterns shown are first-order patterns which correspond to the minimum inter-cell distance a ; if the x axis is parallel with the translation vector corresponding to the minimum inter-cell distance, then the distribution shown in Fig. 2(a) is the 100 line, the distribution shown in Fig. 2(b) is the 10 pattern, and the distribution shown in Fig. 2(c) is the first-order pattern.

In each of the three cases the number N is the number of inter-cell distances in a typical linear dimension of the crystal. Thus, in the case of an assemblage of three-dimensional crystals, N is the cube root of the total number of unit cells in each of the crystals and, in the case of an assemblage of two-dimensional arrays, the number N is the square root of the number of unit cells in each of the two-dimensional arrays.

In Fig. 2(a) the peak intensity is proportional to the number N and the width of the line to N^{-1} . In Fig. 2(b) the height of the peak is proportional to $N^{\frac{1}{2}}$ and the width of the distribution to N^{-1} . Finally, in Fig. 2(c) the height of the peak varies only slightly as the number N is increased. Accordingly, the slope of the rising portion of the intensity curve is proportional to N^2 , $N^{\frac{3}{2}}$ and N for the three cases.

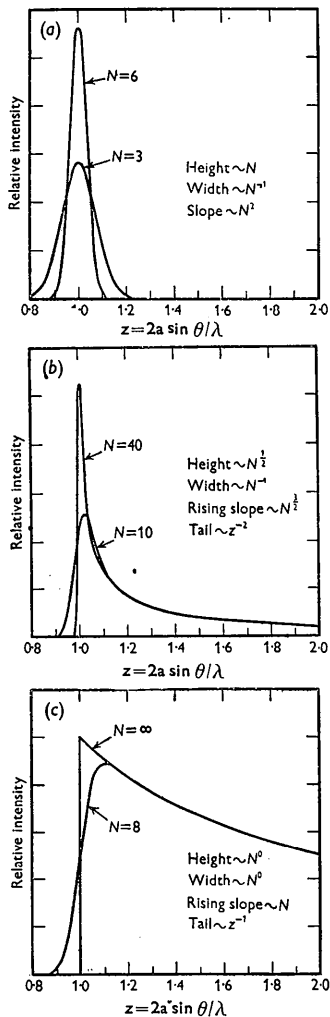


Fig. 2. (a) Three-dimensional crystals. The curves show the relative intensity distribution across a line representing a first-order interference in the powder pattern of a three-dimensional crystal. The abscissa is a dimensionless parameter which involves the corresponding displacement distance a in the crystal. N is the number of inter-cell distances in a typical linear dimension of the crystals. If the total size of the scattering sample is held constant, then the height of the peak is proportional to N and the width at half-maximum to N^{-1} , so that the maximum slope of the rising portion of the curves is proportional to N^2 .

(b) Two-dimensional arrays. The curves show the relative intensity distribution across a line representing a first-order interference in the pattern of randomly oriented two-dimensional arrays. The abscissa is a dimensionless parameter which involves the corresponding displacement distance a in the crystal. N is the number of inter-cell distances in a typical linear dimension of the lattices. If the total size of the scattering sample is held constant, then the height of the peak is proportional to $N^{1/2}$ and the width at half-maximum to N^{-1} , so that the maximum slope of the rising portion of the curves is proportional to $N^{3/2}$.

(c) Line gratings. The curves show the relative intensity distribution of the pattern representing the first-order interference in the pattern of randomly oriented line gratings. The abscissa is a dimensionless parameter which involves the distance a between adjacent unit cells of the line grating. N is the number of unit cells in the line gratings. If the total size of the scattering sample is held constant, then the height of the peak is insensitive to the value of N ; the maximum slope of the rising portion of the curves is proportional to N .

The long tails in the patterns for angles larger than that corresponding to $z=1$ are characteristic of both randomly oriented two-dimensional arrays and randomly oriented line gratings. In the case of the two-dimensional arrays, the intensity in the tail varies as z^{-2} , whereas with the line gratings the intensity in the tail varies as z^{-1} . It is evident that the two-dimensional arrays form a case intermediate between the line gratings and the three-dimensional crystals; the line gratings have no pronounced peak, and the three-dimensional crystals have no tail, whereas the two-dimensional arrays combine both these features in a modified manner.

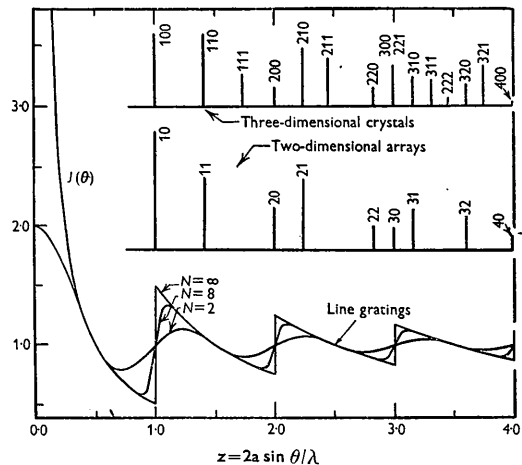


Fig. 3. The three curves in the lowest part of the figure show the function $J(\theta)$, which represents the relative intensity distribution, for randomly oriented line gratings with 2, 8 and an infinite number of unit cells in each line grating. The distance a involved in the definition of z is the inter-cell distance. Note that the maximum slope of the rising parts of the curves is proportional to N . The middle and upper parts of the figure show the positions and relative intensities of the peaks for randomly oriented square lattices, and for randomly oriented simple cubic crystals.

Fig. 3 shows the combined pattern due to all of the orders of a randomly oriented assemblage of line gratings for three different values of N , namely, $N=2$, 8 and ∞ . The points used in plotting these curves are tabulated in Table 2.

It is evident that the overlapping of the various orders is such that it is not in general possible to consider the distribution as due to a single order at a given angle. When N is large, for example, the zero-order pattern contributes one-third of the total intensity between $z=1$ and $z=2$; the zero-order pattern contributes one-fifth of the intensity, and the second and third orders each contribute two-fifths of the total intensity between $z=2$ and $z=3$, and so on.

In order to show another aspect of the relation between the intensity distributions for the three different cases, there have been added to Fig. 3 the positions and relative intensities for the peaks for three-dimensional crystals and two-dimensional arrays. The positions are calculated for a simple cubic lattice and for

Table 2. *The function $J(\theta)$ for $N=2, 8$ and ∞*

z	$J(\theta)$ by approximate eq. (1.5)			$J(\theta)$ by exact	Exact $J(\theta)$ minus
	$N=\infty$	$N=8$	$N=2$	eq. (1.4) $N=2$	approximate $J(\theta)$ $N=2$
0.0	—	8.0000	2.0000	2.0000	0.0000
0.025	—	7.6772	—	—	—
0.050	—	6.8396	—	—	—
0.075	—	5.7827	—	—	—
0.1	5.0000	4.7753	1.9193	1.9355	0.0162
0.125	—	3.9513	—	—	—
0.150	—	3.3246	—	—	—
0.2	2.5000	2.4998	1.7100	1.7568	0.0468
0.3	1.6667	1.6667	1.4464	1.5045	0.0581
0.4	1.2500	1.2500	1.1971	1.2339	0.0368
0.5	1.0000	1.0000	1.0000	1.0000	0.0000
0.6	0.8333	0.8333	0.8686	0.8441	-0.0245
0.7	0.7143	0.7143	0.8087	0.7838	-0.0249
0.8	0.6250	0.6250	0.8225	0.8108	-0.0117
0.850	—	0.5898	—	—	—
0.875	—	0.5784	—	—	—
0.9	0.5556	0.5805	0.8979	0.8961	-0.0018
0.925	—	0.6122	—	—	—
0.950	—	0.6927	—	—	—
0.975	—	0.8288	—	—	—
1.0	0.5000, 1.5000	1.0000	1.0000	1.0000	0.0000
1.025	—	1.1629	—	—	—
1.050	—	1.2731	—	—	—
1.075	—	1.3337	—	—	—
1.1	1.3636	1.3432	1.0836	1.0850	0.0014
1.125	—	1.3279	—	—	—
1.150	—	1.3032	—	—	—
1.2	1.2500	1.2500	1.1183	1.1261	0.0078
1.3	1.1538	1.1538	1.1030	1.1164	0.0134
1.4	1.0714	1.0714	1.0563	1.0668	0.0105
1.5	1.0000	1.0000	1.0000	1.0000	0.0000
1.6	0.9375	0.9375	0.9507	0.9415	-0.0092
1.7	0.8824	0.8824	0.9212	0.9110	-0.0102
1.8	0.8333	0.8333	0.9211	0.9159	-0.0052
1.850	—	0.8115	—	—	—
1.875	—	0.8032	—	—	—
1.9	0.7895	0.8013	0.9516	0.9508	-0.0008
1.925	—	0.8137	—	—	—
1.950	—	0.8503	—	—	—
1.975	—	0.9158	—	—	—
2.0	0.7500, 1.2500	1.0000	1.0000	1.0000	0.0000
2.025	—	1.0824	—	—	—
2.050	—	1.1424	—	—	—
2.075	—	1.1729	—	—	—
2.1	1.1905	1.1798	1.0438	1.0445	0.0007
2.125	—	1.1736	—	—	—
2.150	—	1.1622	—	—	—
2.2	1.1364	1.1364	1.0646	1.0688	0.0042
2.3	1.0870	1.0870	1.0582	1.0658	0.0076
2.4	1.0417	1.0417	1.0329	1.0390	0.0061
2.5	1.0000	1.0000	1.0000	1.0000	0.0000
2.6	0.9616	0.9615	0.9697	1.9640	-0.0057
2.7	0.9259	0.9259	0.9504	0.9439	-0.0065
2.8	0.8929	0.8929	0.9493	0.9460	-0.0033
2.850	—	0.8777	—	—	—
2.875	—	0.8717	—	—	—
2.9	0.8621	0.8698	0.9683	0.9677	-0.0006
2.925	—	0.8774	—	—	—
2.950	—	0.9010	—	—	—
2.975	—	0.9439	—	—	—
3.0	0.8333, 1.1667	1.0000	1.0000	1.0000	0.0000
3.025	—	1.0552	—	—	—
3.050	—	1.0957	—	—	—
3.075	—	1.1167	—	—	—
3.1	1.1290	1.1218	1.0297	1.0302	0.0005
3.125	—	1.1181	—	—	—
3.150	—	1.1107	—	—	—
3.2	1.0938	1.0937	1.0444	1.0473	0.0029
3.3	1.0606	1.0606	1.0406	1.0459	0.0053
3.4	1.0294	1.0294	1.0232	1.0275	0.0043
3.5	1.0000	1.0000	1.0000	1.0000	0.0000
3.6	0.9722	0.9722	0.9781	0.9740	-0.0041
3.7	0.9459	0.9459	0.9638	0.9591	-0.0047
3.8	0.9211	0.9211	0.9626	0.9602	-0.0024
3.850	—	0.9094	—	—	—
3.875	—	0.9048	—	—	—
3.9	0.8974	0.9032	0.9764	0.9760	-0.0004
3.925	—	0.9086	—	—	—
3.950	—	0.9261	—	—	—
3.975	—	0.9580	—	—	—
4.0	0.8750, 1.1250	1.0000	1.0000	1.0000	0.0000

a simple square array, respectively, in both of which the unit cell contains only one atom. Just as in the case of the pattern for the line gratings, the relative intensities do not include the effect of the polarization factor or the structure factor.

It is evident that in the case of both three-dimensional crystals and two-dimensional arrays the lines become more closely spaced as z increases, whereas in the case of the line gratings the various orders are uniformly spaced. It may be shown that the asymptotic density of the lines for the first two cases is proportional to z^2 and z , respectively.

When N is large the expression (1.5) for $J(\theta)$ is much more convenient to use than (1.4). Accordingly, it is desirable to obtain some estimate of the error involved in the use of (1.5). In order to study this question, $J(\theta)$ was calculated from both of the expressions for $N=2$. Evidently this is the most severe test of (1.5), since its accuracy increases as N increases. The two functions are tabulated in Table 2; and the difference between the two functions is also tabulated. It is evident that the difference between them is very small; the maximum difference is about 0.06, and this difference is equal to about 4% of the value itself.

In the case of the three-dimensional crystals and the two-dimensional arrays the width of the peaks at half-maximum intensity affords a convenient means of measuring the number N , which in turn determines the size of the crystals. Because randomly oriented line gratings do not provide a peak whose width is a sensitive function of the number N , it is necessary to use some other method for the case of line gratings.

The method proposed involves measuring the slope of the rising portions of the pattern. A plot of $zJ(\theta)$ has the form shown in Fig. 4, in which the risers of the stairway have a slope which is proportional to N . Now let $\Delta\theta$ be the range of Bragg angles within which the function $zJ(\theta)$ rises from 25% to 75% of the distance between the horizontal treads of the stairway. This range of Bragg angles corresponds to the range of the argument of the error function in which its value rises from 0.25 to 0.75; by inspection of Table 1 this range is 0.954. It follows from (1.8) that the corresponding range in the parameter z is equal to $0.538/N$. It then further follows from (1.3) that the corresponding breadth $B \equiv 2\Delta\theta$ is related to $L \equiv Na$ by

$$L = 0.538\lambda/B \cos \theta \quad (\text{line gratings}). \quad (1.10)$$

The determination of L from the observed intensity pattern may accordingly be accomplished as follows. The observed pattern should first be corrected for the effects of the polarization factor and the structure factor, and, secondly, it should be multiplied by $\sin \theta$. A plot of the resulting pattern versus θ will then have the general form shown in Fig. 4, from which the value of $\Delta\theta$ may easily be determined.

The expression (1.10) for randomly oriented line gratings may be compared with the corresponding

relations for three-dimensional crystals and two-dimensional arrays:

$$L = 0.92\lambda/B \cos \theta \quad (\text{three-dimensional crystals}), \quad (1.11)$$

$$L = 1.84\lambda/B \cos \theta \quad (\text{two-dimensional arrays}), \quad (1.12)$$

where, in the last two relations, $B \equiv 2\Delta\theta$ corresponds to the width of the distribution, as measured between the points where the intensity has dropped to one-half the peak intensity.

The results stated above hold for a gas of identical molecules, each of the molecules being a linear arrangement of identical unit cells which are identically oriented. For the special case in which each of the unit cells contains but a single atom, so that the molecule is a linear molecule containing N identical atoms, the results are in accord with those of Pirene (1946, Chapter 6).

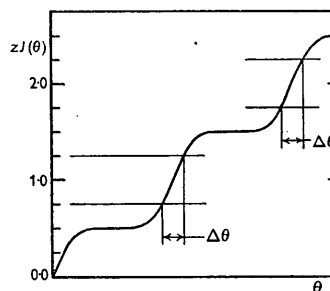


Fig. 4. This is the type of figure which should be drawn in order to determine $\Delta\theta$, and thereby L , from densitometer curves, as described in Part I.

Part II. Derivation of results*

The exact expression for $J(\theta)$ in the form (1.4) may be obtained very simply from a general result of Debye (1915). In the notation used in this paper, Debye has shown that the general result for the function $J(\theta)$ for any type of randomly oriented crystal is given by

$$J(\theta) = \frac{1}{N} \sum_{k,l} \frac{\sin 2\pi z_{kl}}{2\pi z_{kl}}, \quad (2.1)$$

where the indices k and l are to run separately over the unit cells in the crystal, where N is the total number of unit cells in the crystals, and where z_{kl} is defined by

$$z_{kl} = (2r_{kl}/\lambda) \sin \theta. \quad (2.2)$$

The quantity r_{kl} is the distance between the unit cells designated by k and l . The expression (1.4) for randomly oriented line gratings may now be obtained directly from (2.1) by noting that there are just N terms in (2.1) for which r_{kl} is zero, that there are just $2(N-1)$ terms for which r_{kl} equals a , just $2(N-2)$ for which r_{kl} equals $2a$, and so on.

* The original manuscript of this paper contained a straightforward derivation of equation (1.2) from first principles, but at the suggestion of the Editor this derivation has been omitted from the present paper for the sake of brevity. A few copies of the original manuscript are available and may be obtained by writing to the author.

The result (1.4) has thus been established. The expression for $J(\theta)$ in the form (1.2) may be obtained from (1.4) by a purely mathematical transformation. Because the transformation is not obvious, and because the writer is not aware of any publication where a proof of the transformation may be found, a derivation is provided in the Appendix.

The approximate expression (1.5) for the function $J(\theta)$ may be obtained from (1.2) by use of the approximation

$$\frac{\sin^2 Nx}{\sin^2 x} \doteq N^2 \sum_h \exp[-(N^2/\pi)(x - \pi h)^2], \quad (2.3)$$

where h assumes all integral values, positive, negative and zero, and by the use of the further approximation of replacing the lower limit of each of the resulting integrals (except the one for $h=0$) by minus infinity.

This completes the derivation of the results given in Part I.

The expression (1.2) for $J(\theta)$ is not correct for very small values of θ . This fact may be seen in the following way:

As z approaches zero, $J(\theta)$ approaches the value N :

$$\lim_{z=0} J(\theta) = N. \quad (2.4)$$

The substitution of this expression in (1.1) then leads to the conclusion that the intensity scattered at very small angles is proportional to $N^2 M$, whereas it follows from fundamental considerations that at very small angles the scattered intensity must be proportional to $N^2 M^2$. This discrepancy arises from the assumption that the line gratings are randomly arranged in space. When the angle θ becomes smaller than $\lambda/2\mathcal{L}$, where \mathcal{L} is the transverse linear dimension of the sample, it is no longer possible to ignore the correlation between the positions of the separate line gratings. At angles small compared with $\lambda/2\mathcal{L}$, the waves scattered from all of the line gratings will add up in phase. A detailed consideration of this fact leads to the introduction of an extra factor M ; this introduction removes the discrepancy.

The writer wishes to thank Dr Cutler D. West, Polaroid Corporation, for suggesting the problem treated here. He is further indebted to both Prof. B. E. Warren and Dr West for helpful discussions, and he wishes to thank Mr Samuel Stone for checking all of the mathematical derivations in this paper and for supplying the proof given in the Appendix.

Appendix

This section contains a proof of the identity of f and g , where

$$f \equiv \int_0^z \frac{\sin^2 Nx}{\sin^2 x} dx, \\ g \equiv Nz + \sum_{i=1}^{N-1} \frac{N-i}{i} \sin 2iz.$$

The writer's first acquaintance with the integral f occurred in 1942 in connection with the signal-to-noise ratio of hydrophone arrays. At that time, the writer proposed and used the identity of f and g for all values of N on the basis of proofs only for $N=1, 2, 3$ and 4 ; the identity was later proved for all values of N by Mr C. E. Shannon, of Bell Telephone Laboratories, by a generalized method of mathematical induction. The following proof by direct derivation was worked out in 1947 by Mr Samuel Stone, formerly of the Polaroid Corporation.

The starting point of the derivation is the relation (Dwight, 1934, p. 79)

$$\sum_{i=0}^{N-1} \sin(\alpha - 2ix) = \frac{\sin Nx \sin[\alpha - (N-1)x]}{\sin x}, \quad (1)$$

where α is arbitrary. By use of the substitution

$$\alpha = (N-1)x + \frac{1}{2}\pi, \quad (2)$$

equation (1) becomes

$$\frac{\sin Nx}{\sin x} = \sum_{i=0}^{N-1} \cos[(N-1-2i)x], \quad (3)$$

whence

$$\frac{\sin^2 Nx}{\sin^2 x} = \sum_{i,j=0}^{N-1} \cos[(N-1-2i)x] \cos[(N-1-2j)x]. \quad (4)$$

Upon integration one finds

$$f = \int_0^z \frac{\sin^2 Nx}{\sin^2 x} dx \\ = \frac{1}{2} \sum_{i,j=0}^{N-1} \left\{ \frac{\sin 2(i-j)z}{2(i-j)} + \frac{\sin 2(N-1-i-j)z}{2(N-1-i-j)} \right\} \quad (5)$$

$$= \sum_{i,j=0}^{N-1} \frac{\sin 2(i-j)z}{2(i-j)}. \quad (6)$$

An enumeration of the number of terms in the last summation for which $i-j=k$ yields $N-|k|$. The last expression therefore becomes

$$f = Nz + 2 \sum_{k=1}^{N-1} (N-k) \frac{\sin 2kz}{2k}. \quad (7)$$

This completes the derivation.

References

- COMPTON, A. H. & ALLISON, S. K. (1935). *X-rays in Theory and Experiment*. New York: van Nostrand.
- DEBYE, P. (1915). *Ann. Phys., Lpz.*, **46**, 809.
- DWIGHT, H. B. (1934). *Tables of Integrals*. London: Macmillan.
- PIRENNE, M. H. (1946). *The Diffraction of X-rays and Electrons by Free Molecules*. Cambridge: University Press.
- WARREN, B. E. (1941). *Phys. Rev.* **59**, 693.